THE JOURNAL OF BIOLOGICAL CHEMISTRY
Vol. 278, No. 46, Issue of November 14, pp. 45931–45936, 2003
Printed in U.S.A.

Endocytosis of Oxidized Low Density Lipoprotein through Scavenger Receptor CD36 Utilizes a Lipid Raft Pathway That Does Not Require Caveolin-1*

Received for publication, July 17, 2003, and in revised form, August 20, 2003
Published, JBC Papers in Press, August 28, 2003, DOI 10.1074/jbc.M307722200

Youchun Zeng‡, Nengbing Tao‡§, Koong-Nah Chung¶, John E. Heuser¶, and Douglas M. Lublin‡‖

From the ‡Department of Pathology, Division of Laboratory Medicine, and ¶Department of Cell Biology and Physiology, Washington University School of Medicine, St. Louis, Missouri 63110

The scavenger receptor CD36 binds a diverse array of ligands, including thrombospondin-1, oxidized low density lipoprotein (OxLDL), fatty acids, anionic phospholipids, and apoptotic cells. CD36 has been reported to be present in lipid rafts/caveolae, but little is known about the membrane trafficking of this protein at baseline or following ligand binding. Here, we determined that expression of CD36 in Chinese hamster ovary (CHO) cells and endogenous expression of CD36 in C32 cells led to a homogeneous distribution of the protein on the plasma membrane, as judged by confocal fluorescence microscopy. This homogeneous pattern was observed both by anti-CD36 antibody staining and by live cell imaging of CHO cells expressing a chimeric CD36-green fluorescent protein construct. In contrast, caveolin-1 displayed its usual punctate surface distribution. Correspondingly, dual labeling of CD36 and caveolin-1 showed essentially no overlap, neither by immunofluorescence light microscopy nor by immunogold electron microscopy. Furthermore, isolation of lipid rafts by sucrose gradient ultracentrifugation of cold Triton X-100 cell lysates yielded both CD36 and caveolin-1, but immunoprecipitates of caveolin-1 did not contain CD36. Binding of OxLDL led to internalization of CD36 and OxLDL into endosomal structures that did not contain caveolin-1 or transferrin but that co-internalized the glycosyl-phosphatidylinositol-anchored protein decay accelerating factor, a lipid raft protein. Furthermore, expression of CD36 in the caveolin-1-negative KB cell line is sufficient for OxLDL-induced internalization of CD36, indicating that caveolin-1 is not required for this endocytic process. Taken together, these data demonstrate that at steady state, CD36 is localized in lipid rafts but not in caveolae, and that binding of OxLDL to CD36 leads to endocytosis through a lipid raft pathway that is distinct from the clathrin-mediated or caveolin internalization pathways.

CD36 is an 88-kDa plasma membrane glycoprotein that functions as a scavenger receptor. It is expressed in a range of cells and tissues that includes platelets (1), monocytes/macrophages (2), mammary epithelial cells (3), vascular endothelial cells (4), and adipose tissues (5). A large and diverse array of ligands for CD36 has been identified, including thrombospondin (6), oxidized low density lipoprotein (OxLDL)[1] (7, 8), fatty acids (5), anionic phospholipids (9), apoptotic cells (10, 11), and *Plasmodium falciparum* malaria-parasitized erythrocytes (12). This set of CD36 ligands suggests possible roles for CD36 in a range of important physiologic and pathologic processes, including angiogenesis, phagocytosis, lipid metabolism, and atherosclerosis (reviewed in Ref. 13).

Binding of OxLDL to macrophages is one of the earliest steps in development of atherosclerotic lesions, producing lipid-laden foam cells (reviewed in Ref. 14). CD36 is one of several OxLDL receptors that have been implicated in this process. Monocytes from individuals lacking CD36 (Nak^a -negative, type I deficiency) or monocytes in which CD36 is blocked by antibodies have a decrease of ~50% in OxLDL uptake (7, 8, 15); a similar decrease is seen in macrophages from CD36 knockout mice compared with control CD36-positive litter mates (16). When studied in a proatherogenic apoE-null background, the CD36 knockout resulted in a 75% reduction in aortic atherosclerotic lesion size compared with control animals (16). These data support the critical role of CD36 as a proatherogenic molecule.

Despite the pathophysiologic importance of the pathway for uptake of OxLDL through CD36, the molecular details of the endocytosis of OxLDL into macrophages to form foam cells is not well understood. Initial observations localized CD36 to lipid rafts/caveolae (17). Rafts are membrane domains that are enriched in cholesterol and sphingolipids and form a liquid-ordered subdomain of the membrane (reviewed in Refs. 18 and 19). Rafts contain a select set of membrane proteins, including glycosyl-phosphatidylinositol (GPI)-anchored proteins and acylated src family protein-tyrosine kinases. Rafts are found in all cells; caveolae are a specialized raft subdomain found in some cells (reviewed in Ref. 20). Caveolae are 50- to 100-nm plasma membrane invaginations that have the coat protein caveolin-1 (21). Expression of the protein caveolin-1 in cells that lack caveolae leads to formation of structural caveolae (22); conversely, caveolae are lost in the caveolin-1 knockout mouse (23, 24).

Rafts can be purified as detergent-resistant membranes (DRMs) based on their resistance to extraction in Triton X-100 at 4 °C, followed by subsequent separation from the remainder

* This work was supported in part by National Institutes of Health Grant GM41297 (to D. M. L.), and part of this work was done during the tenure of a grant-in-aid from the American Heart Association and Pfizer, Inc. (to D. M. L.). The costs of publication of this article were defrayed in part by the payment of page charges. This article must therefore be hereby marked "*advertisement*" in accordance with 18 U.S.C. Section 1734 solely to indicate this fact.

§ Supported by National Institutes of Health Training Grant T32-HL07038.

‖ To whom correspondence should be addressed: Dept. of Pathology, Washington University School of Medicine, 660 S. Euclid Ave., Box 8118, St. Louis, MO 63110. Tel.: 314-362-8849; Fax: 314-362-3016; E-mail: lublin@pathbox.wustl.edu.

[1] The abbreviations used are: OxLDL, oxidized low density lipoprotein; CHO, Chinese hamster ovary cells; GPI, glycosyl-phosphatidylinositol; DRM, detergent resistant membrane; DAF, decay accelerating factor; SR-A, scavenger receptor class A; IL-2, interleukin-2; GFP, green fluorescent protein; Mes, 4-morpholineethanesulfonic acid; PBS, phosphate-buffered saline; DiI, 1,1′-dioctadecyl-3,3,3′,3′-tetramethylindocarbocyanine.

of the solubilized membrane proteins due to their high lipid content and resultant light buoyant density, which leads to flotation on sucrose gradient ultracentrifugation (25, 26). CD36 was identified as a caveolar protein based on its partitioning into this DRM fraction, but this methodology does not distinguish caveolae from non-caveolar rafts. Hence, CD36 is enriched in rafts, but it remains to be determined whether it is in caveolae. Furthermore, it is not known whether rafts and caveolae play a role in the endocytosis of ligands such as Ox-LDL through CD36. The studies reported here address the localization of CD36 to rafts and/or caveolae and assess changes in that distribution following OxLDL binding and endocytosis.

EXPERIMENTAL PROCEDURES

Cells and Antibodies—Chinese hamster ovary (CHO) cells were grown in Ham's F-12 medium supplemented with 5% fetal bovine serum, 2 mM glutamine, and 10 μg/ml streptomycin, and 10 units/ml penicillin in a 5% CO_2/95% air atmosphere at 37 °C. A stable CHO transfectant expressing human decay accelerating factor (DAF) has been described previously (27). The human KB cell line and the human C32 melanoma cell line were grown in α-minimal essential medium supplemented with 10% fetal bovine serum plus the remaining listed additions, and the J774 mouse macrophage cell line was grown in Iscove's minimal essential medium supplemented with 10% fetal bovine serum with the same additions; these cell lines were all obtained from the American Type Culture Collection (Rockville, MD). Mouse monoclonal anti-CD36 antibody FA6–152 was obtained from Immunotech (Westbrook, ME), rabbit polyclonal anti-caveolin-1 antibody and mouse monoclonal anti-caveolin-2 antibody were purchased from BD Transduction Laboratories (Lexington, KY), and the anti-FLAG monoclonal antibody M2 was from Sigma (St. Louis, MO). The mouse monoclonal anti-human DAF antibody 1H4 has been described previously (28). Secondary antibodies (anti-rabbit IgG and anti-mouse IgG) were from Jackson ImmunoResearch Laboratories (West Grove, PA), horseradish peroxidase-conjugated secondary antibodies were from Sigma, and Alexa 488- and Alexa 594-conjugated secondary antibodies and Alexa 488-conjugated transferrin were from Molecular Probes (Eugene, OR).

DNA Constructs and Transfection—Human CD36 cDNA was cloned into the pcDNA3 expression vector (Invitrogen, Carlsbad, CA) as previously reported (29). The PCR was used to place the FLAG epitope tag at the C terminus of CD36 just before the stop codon. A chimeric construct with green fluorescent protein (GFP) at the N terminus of CD36 (CD36-GFP) was made by cloning the CD36 cDNA from the pcDNA3 vector into the pEGFP-C1 vector (Clontech Laboratories, Palo Alto, CA) utilizing HindIII and ApaI restriction sites. Canine caveolin-1 cDNA was cloned into the pcDNA3 expression vector as previously described (30). A chimeric construct with GFP at the C terminus of caveolin-1 (Cav-1-GFP) was made by cloning caveolin-1 cDNA from the pcDNA3 vector into pEGFP-N1 as a XhoI/HindIII fragment. DNA transfection was performed with LipofectAMINE Plus (Invitrogen, Gaithersburg, MD) for 4 h at 37 °C. Cells were either studied during transient expression at 24–48 h post-transfection, or stable transfectants were selected in medium containing 250 μg/ml G418 (active drug). In some cases, stable transfectants were further enriched for high expression levels by flow cytometry or cloning by limiting dilution.

Sucrose Gradient Ultracentrifugation—Rafts were purified as DRMs using sucrose gradient ultracentrifugation (25) as modified (26). In brief, 50–100 $\times$ 10^6 cells were lysed on ice for 30 min in 1 ml of Mes-buffered saline (MBS, 25 mM Mes, pH 6.5, 0.15 M NaCl, 5 mM EDTA, 1 mM sodium orthovanadate, 10 μg/ml leupeptin, and 10 μg/ml aprotinin) containing 0.5% Triton X-100. Cell lysate was brought to 40% sucrose and placed at the bottom of an ultracentrifugation tube, and a 5–30% discontinuous sucrose gradient (in MBS) was laid on top of it and centrifuged at 39,000 rpm at 4 °C for 16 h in a SW41 rotor (Beckman Instruments, Palo Alto, CA). 1-ml fractions were collected from the top of the tube to yield a total of 10 fractions. 5% of each fraction was analyzed by SDS-PAGE and Western blotting.

Immunoprecipitation and Western Blotting—Cells were washed twice with phosphate-buffered saline (PBS, pH 7.4) and lysed in lysis buffer (50 mM Tris-HCl, pH 7.6, 0.15 M NaCl, 1%Triton X-100, 5 mM EDTA, 1 mM sodium orthovanadate, 10 μg/ml leupeptin, and 10 μg/ml aprotinin). For immunoprecipitation, lysates or fractions from sucrose gradient ultracentrifugation were precleared with secondary antibody and the immunoabsorbent Pansorbin (Calbiochem, San Diego, CA). CD36 was immunoprecipitated with a mouse monoclonal antibody (FA6–152) and rabbit anti-mouse IgG, and caveolin-1 was immunoprecipitated with rabbit anti-caveolin-1. Immunoprecipitates were collected on Pansorbin, washed three times in lysis buffer, and eluted into Laemmli sample buffer. Cell lysates or immunoprecipitates were separated by SDS-PAGE on 9% or 12% acrylamide gels, and proteins were transferred to a 0.45-μm nitrocellulose membrane (Micron Separations, Westboro, MA) and blocked for 30 min in blocking buffer (Tris-buffered saline, pH 7.6, 0.05% Tween, and 3% nonfat dry milk). After a 60-min incubation with primary antibody diluted in blocking buffer followed by washing, the blot was incubated for 30 min with appropriate secondary anti-IgG-horseradish peroxidase conjugate. The membrane was washed three times for 10 min each and developed with SuperSignal chemiluminescent substrate (Pierce, Rockford, IL).

Confocal Fluorescence Microscopy—Cells (5 $\times$ 10^4 cells/well) were plated on chromic acid-cleaned glass 22 mm-square coverslips that were put into 35-mm wells, and 24 h later they were transfected. Following a further 24- to 48-h incubation, cells were fixed and stained for immunofluorescence at room temperature. In detail, cells were washed twice with PBS, fixed for 60 min with 3.7% paraformaldehyde in PBS, rinsed three times (10 min each) with PBS, permeabilized for 20 min with Blocker 1 (PBS, 0.1 M NH_4Cl, 0.2% gelatin, and 0.05% Triton X-100), rinsed three times (5 min each) in wash buffer (PBS, 0.02% azide, and 0.2% gelatin), incubated with primary antibody (or two primary antibodies for dual immunofluorescence), either rabbit anti-caveolin-1 antibody and/or mouse monoclonal anti-CD36 antibody FA6–152 (both at 1:100 dilution) in wash buffer plus 25% normal goat serum for 1 h, rinsed in wash buffer four times (for a total of 30 min), incubated with secondary Alexa Fluor 488- and/or Alexa Fluor 594-conjugated goat anti-IgG in wash buffer plus 25% normal goat serum for 1 h in the dark, and rinsed in wash buffer four times for a total of 30 min. All samples were mounted and viewed using a Bio-Rad laser confocal fluorescence microscope. The specificity of the primary antibodies was confirmed by the lack of fluorescence after staining of antigen-negative cell lines.

Cryo-immunogold Electron Microscopy—Cells were grown to ~80% confluency in each of two 10-cm plates. Cells were rinsed twice with PBS, harvested with PBS and 10 mM EDTA, and rinsed twice with PBS. The cell pellet was prepared for cryo-sections by fixing with 2% paraformaldehyde and 0.2% glutaraldehyde in PBS. Cryo-sections were floated onto grids and labeled with 1:100 dilution of polyclonal rabbit anti-caveolin-1 and 1:100 dilution of monoclonal anti-CD36 (FA6–152), and secondary anti-rabbit IgG-gold (10-nm gold, Jackson Laboratories) and anti-mouse IgG-gold (5-nm gold, Jackson Laboratories) as described previously (31).

Ligand Binding—Cells were plated in six-well dishes on coverslips and, when indicated, transfected as described above. Antibody binding was done using FA6–152 anti-CD36 or 1H4 anti-DAF at 2 μg/ml for 30 min at 37 °C followed by addition of rabbit anti-mouse IgG (either unlabeled or a fluorophore-conjugated antibody) at 10 μg/ml for 30 min at 37 °C. Ligand binding was done by incubation with OxLDL or DiI-OxLDL (Intracel, Frederick, MD) at 20 μg/ml for 30–60 min at 37 °C. Following these incubations, the cells were fixed, stained with antibody if indicated, and mounted for viewing by confocal fluorescence microscopy. In some cases, ligand binding was done in the presence of fucoidan or polyinosinic acid at 200 μg/ml (Sigma).

RESULTS

CD36 Is in Lipid Rafts Distinct from Caveolae—Immunofluorescence microscopy was used to address the localization of CD36 relative to caveolae in cells at steady state, *i.e.* cells without ligand activation of CD36. Chinese hamster ovary (CHO) cells endogenously express caveolin-1 and form caveolae (data not shown), and caveolin-1 can be used as a marker of caveolae location. CHO stable transfectants expressing CD36 were established. Analysis of these cells by immunofluorescence using separate antibodies to CD36 or caveolin-1 demonstrated that both CD36 and caveolin-1 were localized at the plasma membrane (Fig. 1). This is clearly seen in a confocal optical section through the middle of the cell (Fig. 1, *C* and *D*). A confocal plane at the cell bottom (Fig. 1, *A* and *B*) demonstrated a punctate pattern for caveolin-1, as expected for the coat protein of caveolae, but showed a quite different appearance for CD36 with a smooth, homogeneous pattern. Next, studies were performed to confirm that these patterns were not artifactually modified by the antibodies used for immunofluorescence (which are applied post-paraformaldehyde fixation) or

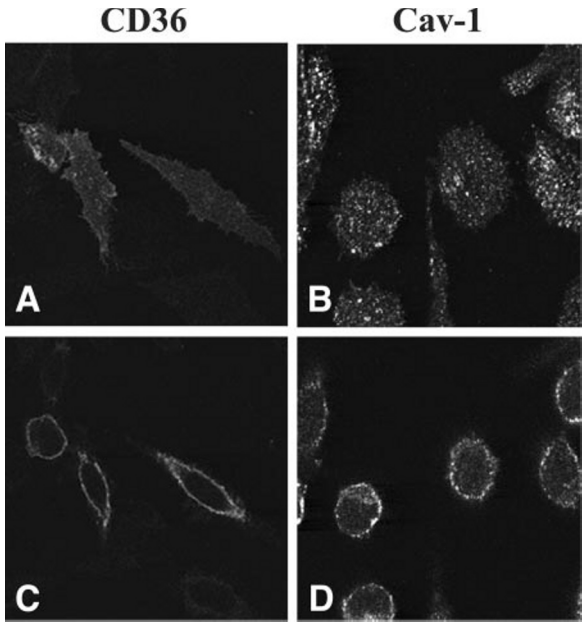

FIG. 1. **Immunofluorescence analysis of CD36 and caveolin in CHO cells.** CHO cells stably transfected with CD36 were stained with either anti-CD36 monoclonal antibody FA6–152 (*A* and *C*) or anti-caveolin-1 rabbit polyclonal antibody (*B* and *D*), followed by Alexa 488-conjugated goat anti-mouse IgG or goat anti-rabbit IgG, respectively. Each set of cells is shown in a confocal plane through the cell bottom (*A* and *B*) or through the middle of the cell (*C* and *D*).

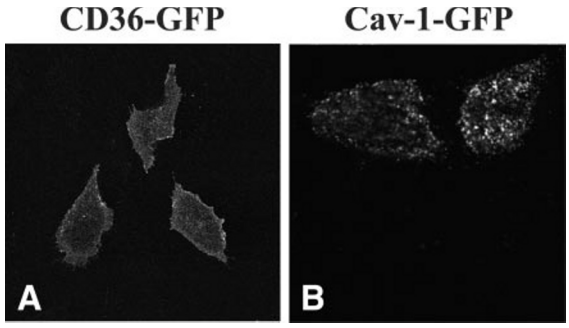

FIG. 2. **Expression of GFP-tagged versions of CD36 or caveolin-1 in CHO cells.** CHO cells transiently transfected with CD36-GFP (*A*) or caveolin-1-GFP (*B*) were viewed by confocal fluorescence microscopy in a plane near the cell bottom. Note that the GFP tag does not alter the expression pattern of the molecules (compare Fig. 1*A* to Fig. 2*A* for CD36, and Fig. 1*B* to Fig. 2*B* for caveolin-1).

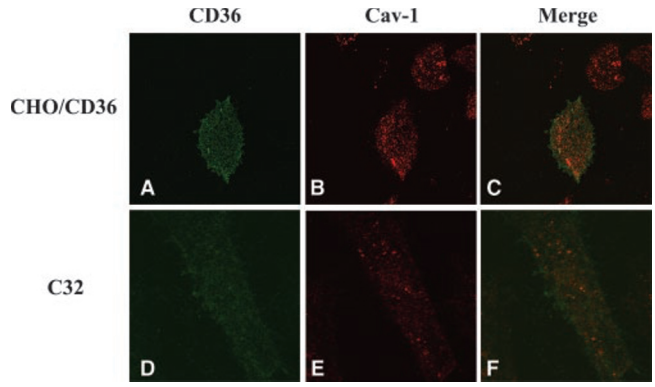

FIG. 3. **CD36 and caveolin-1 do not colocalize in CHO cells or C32 cells as assessed by dual confocal immunofluorescence microscopy.** CHO cells were transiently transfected with CD36-GFP, and 48 h later they were fixed and stained with anti-caveolin-1 rabbit polyclonal antibody, followed by Alexa 594 goat anti-rabbit IgG. C32 cells were fixed, stained with both anti-CD36 monoclonal and anti-caveolin-1 polyclonal antibody, followed by Alexa 488 goat anti-mouse IgG and Alexa 594 goat anti-rabbit IgG. Each set of cells is shown in a confocal plane through the cell bottom: CHO cells (*A–C*) and C32 cells (*D–F*). The CD36 fluorescence is shown in *A* and *D*, the caveolin-1 fluorescence is shown in *B* and *E*, and the merged images are shown in *C* and *F*.

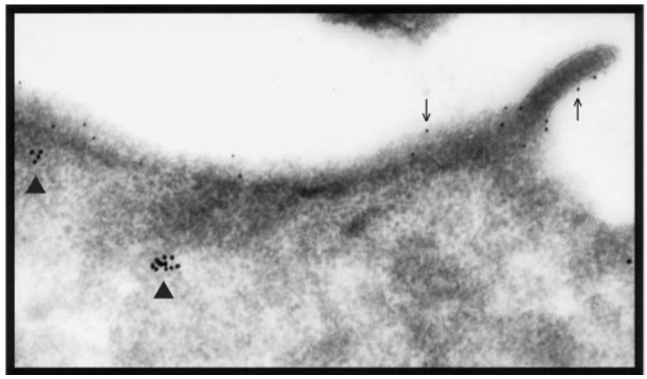

FIG. 4. **Cryo-immunogold electron microscopy of CD36 and caveolin-1 in CHO cells.** CHO cells stably transfected with CD36 were double labeled with monoclonal anti-CD36 antibody FA6–152 and rabbit polyclonal anti-caveolin-1 antibody, followed by gold-labeled secondary antibodies; 5-nm gold particles identify CD36 (marked with *arrows*) and 10-nm gold particles identify caveolin-1 (marked with *arrowheads*).

by the fixation procedure. The patterns of expression observed in CHO cells transiently transfected with plasmids for CD36-GFP or Cav-1-GFP (fixed cells, Fig. 2; live cells, data not shown) were consistent with the immunofluorescence observations. Because the CD36 molecule is expressed by transfection is these CHO cells, it is important to ascertain that the same patterns of expression would occur in cells that endogenously express CD36. The human C32 melanoma cell line expresses CD36 as assessed by flow cytometry (32) and by immunoblot analysis (data not shown), and expresses caveolin-1 as assessed by immunoblot analysis (data not shown). Immunofluorescence analysis demonstrated a smooth, homogeneous pattern of expression of CD36 on the plasma membrane of C32 cells, clearly differing from the punctate plasma membrane expression of caveolin-1 (data not shown).

The distinct patterns of expression of CD36 and caveolin-1 suggest that these two proteins are not colocalized in these cells. To directly confirm this finding, we used dual immunofluorescence of CD36 and caveolin-1 in the same cell. For both CHO stable transfectants expressing CD36 and C32 cells endogenously expressing CD36, the CD36 had a homogeneous staining pattern and caveolin-1 had a more punctate appearance by immunofluorescence, with little overlap in the merged images (Fig. 3).

Next, to completely resolve this issue, we assessed the colocalization of CD36 and caveolin-1 at higher resolution using electron microscopy. Cryo-immunogold electron microscopy of CHO-stable transfectants expressing CD36 showed a distinct localization of CD36 and caveolin-1 (Fig. 4). Caveolin-1 was present in clusters, consistent with its known oligomerization properties and its localization in caveolae (20). The great majority of the CD36 is diffusely located along the plasma membrane and is very rarely seen in a caveolin-1 cluster. Thus, based on both immunofluorescence and immunoelectron microscopy, CD36 and caveolin-1 have distinct and non-overlapping distributions on the plasma membrane in CHO and C32 cells.

CD36 and Caveolin-1 Are in Separate DRMs—Next, to complement these microscopy studies, we did a biochemical analysis of the CD36 and caveolin-1. The original assignment of

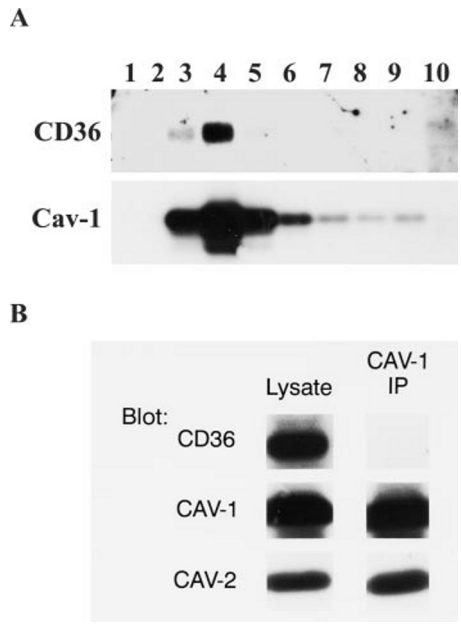

FIG. 5. **CD36 and caveolin-1 are both in rafts, but they do not coimmunoprecipitate.** CHO cell transfectants stably expressing CD36 were lysed in cold 1% Triton X-100, and the lysate was resolved on a sucrose density gradient by ultracentrifugation. *A*, *fractions 1–10* (*fraction 1* at top of gradient) were collected, separated by SDS-PAGE, and analyzed by Western blot for CD36 or caveolin-1. Both CD36 and caveolin-1 are in the DRM (raft) fractions. *B*, the Triton lysate was immunoprecipitated for caveolin-1, and the lysate or immunoprecipitate was separated by SDS-PAGE and analyzed by Western blot for CD36, caveolin-1, or caveolin-2. Note that the caveolin-1 immunoprecipitate contains caveolin-1 and caveolin-2 (which hetero-oligomerizes with caveolin-1), but not CD36.

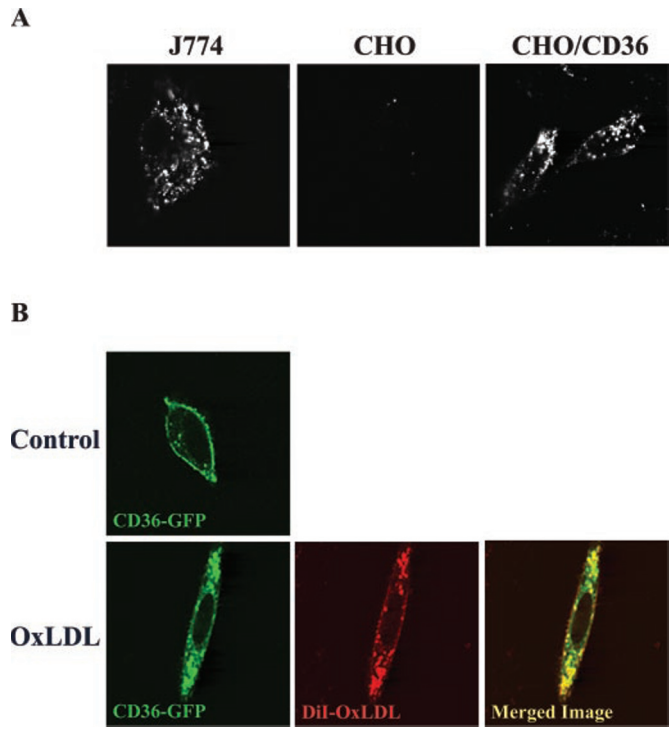

FIG. 6. **DiI-OxLDL is internalized in the J774 macrophage cell line and in CHO cell transfectants stably expressing CD36.** *A*, J774 cells, CHO cells, and CHO cell transfectants stably expressing CD36 were treated with DiI-labeled OxLDL at 20 μg/ml for 1 h at 37 °C, then rinsed, fixed, and viewed by confocal fluorescence microscopy in a plane through the middle of the cell. The J774 cells internalize DiI-OxLDL into vesicular structures, and a similar pattern is seen in the CHO cells transfected with CD36, but not in the CHO cells. *B*, CHO cells were transfected with CD36-GFP, then, following a 48-h incubation, the cells were treated with either buffer (control) or DiI-labeled OxLDL at 20 μg/ml for 1 h at 37 °C, then rinsed, fixed, and viewed by confocal fluorescence microscopy. In a control cells, the CD36-GFP fluorescence is on the plasma membrane, as expected. Following DiI-OxLDL treatment, the CD36-GFP has been internalized along with the DiI-OxLDL, and the *merged image* demonstrates almost complete colocalization.

CD36 as a raft protein was based on biochemical studies isolating CD36 in a light buoyant density fraction from sucrose gradient centrifugation of Triton X-100 cell lysates (17), *i.e.* it partitioned into DRMs, which represent an operational counterpart of rafts (19, 33). Consistent with this finding, when we isolated DRMs from the CHO-stable transfectant expressing CD36, both CD36 and caveolin-1 were found in the DRMs (Fig. 5*A*), identifying both as raft proteins. However, when caveolin-1 was isolated from the Triton X-100 lysate by immunoprecipitation, the immunoprecipitate had no CD36 present as assessed by immunoblot analysis (Fig. 5*B*). Control immunoblots of the caveolin-1 immunoprecipitate confirmed the presence of caveolin-1 and demonstrated the recovery of caveolin-2 (Fig. 5*B*), consistent with the established hetero-oligomeric caveolin-1/caveolin-2 complex (34).

Endocytosis of OxLDL Occurs through CD36 in Transfected CHO Cells—The results above demonstrate that, in the CHO cells at steady state, CD36 is in rafts but is not in caveolae. We next investigated whether the CD36 distribution is affected dynamically by binding of the ligand OxLDL (7). Using DiI-labeled OxLDL for fluorescent visualization of this process, we confirmed that DiI-OxLDL was endocytosed into CHO-stable transfectants expressing CD36 but not into control CHO cells (Fig. 6*A*). Pathophysiologically, the binding and uptake of OxLDL by macrophages is what leads to the formation of foam cells in the early stages of atherosclerosis (14). Therefore, we compared the transfected CHO cells expressing CD36 to the J774 mouse macrophage cell line, and the pattern of OxLDL uptake matched the uptake in the J774 cells (Fig. 6*A*).

The same process of uptake of OxLDL through CD36 was next studied while following both the OxLDL (with a DiI label) and the CD36 (with a GFP tag). A CD36-GFP construct expressed in CHO cells was correctly localized on the plasma membrane (Fig. 6*B*). In the presence of OxLDL, both the OxLDL and the CD36 were internalized, and there was almost complete overlap of the OxLDL and the CD36 molecules, as seen in the merged image (Fig. 6*B*). Thus, the process of OxLDL endocytosis can be studied in this heterologous system of CD36 expressed in CHO cells.

OxLDL Endocytosis Occurs through a Lipid Raft Pathway That Is Clathrin- and Caveolin-1-independent—Several distinct pathways for endocytosis of molecules have been described (35). To characterize the pathway for endocytosis of OxLDL through CD36, we utilized markers for different endocytic pathways and used confocal fluorescence microscopy to assess co-endocytosis with OxLDL. Specifically, transferrin uptake was used to mark the clathrin-mediated pathway, caveolin-1 was used to mark the caveolar pathway, and the GPI-anchored protein DAF was used to mark the lipid raft pathway. CHO cells expressing CD36 were incubated with DiI-OxLDL at 20 μg/ml for 30 min at 37 °C, then the cells were fixed and caveolin-1 was visualized with anti-caveolin-1 and Alexa 488-labeled secondary antibody. Confocal fluorescence microscopy demonstrated that the endocytosed DiI-OxLDL and the caveolin-1 had distinct, non-overlapping localizations (Fig. 7). Similarly, experiments in the C32 cells, which express CD36 endogenously, demonstrated that endocytosed DiI-OxLDL did not colocalize with caveolin-1 (data not shown). Next, to assess whether DiI-OxLDL was internalized via clathrin-coated pits,

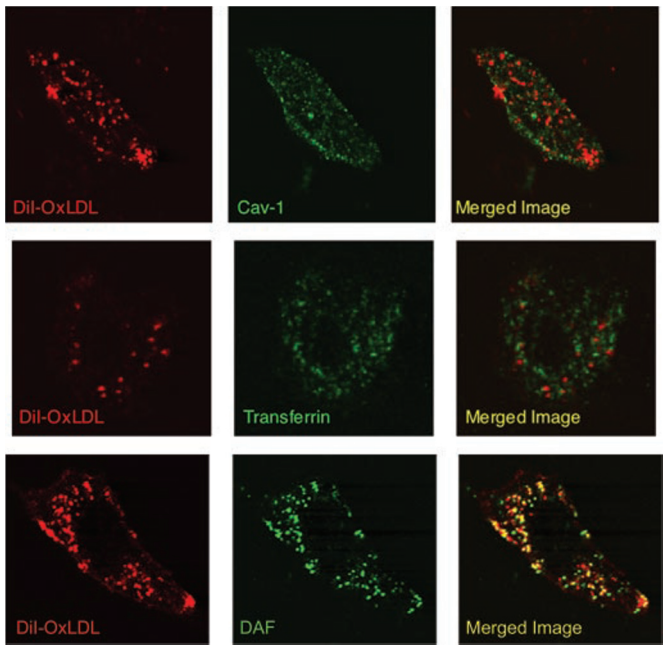

FIG. 7. **Internalized OxLDL does not colocalize with transferrin or caveolin-1 but colocalizes with GPI-anchored DAF.** *Top panels*: CHO cells stably expressing CD36 were transiently transfected with cav-1-GFP, and 24 h later they were treated with DiI-labeled OxLDL at 20 μg/ml for 1 h at 37 °C, then rinsed, fixed, and viewed by confocal fluorescence microscopy. Cells were imaged for DiI-OxLDL, cav-1-GFP, or both (*merged image*), as indicated. *Middle panels*: CHO cells stably expressing CD36 were treated with DiI-labeled OxLDL at 20 μg/ml and with Alexa 488-labeled transferrin for 30 min at 37 °C, then rinsed, fixed, and viewed by confocal fluorescence microscopy. Cells were imaged for DiI-OxLDL, transferrin, or both (*merged image*), as indicated. *Bottom panels*: CHO cells stably expressing the GPI-anchored protein DAF were transiently transfected with CD36, and 48 h later they were pre-treated with 1H4 mouse monoclonal anti-DAF followed by Alexa 488-labeled goat anti-mouse antibody and DiI-labeled OxLDL at 20 μg/ml for 60 min at 37 °C, then rinsed, fixed, and viewed by confocal fluorescence microscopy.

the transfected CHO cells expressing CD36 were incubated with DiI-OxLDL and Alexa 488-labeled transferrin, because the transferrin will be internalized through clathrin-coated pits and vesicles. The cells were fixed and viewed by confocal fluorescence microscopy (Fig. 7), which showed that both the DiI-OxLDL and the transferrin had been endocytosed, but that they were in distinct vesicles, with no overlap. Finally, possible endocytosis of OxLDL along the lipid raft pathway was studied in a CHO-stable DAF transfectant that was transiently expressing CD36. These cells were incubated with 1H4 monoclonal antibody to DAF at 4 °C, followed by Alexa 488-labeled secondary antibody and DiI-OxLDL at 20 μg/ml for 30 min at 37 °C. Cells were fixed and viewed by confocal fluorescence microscopy, which demonstrated that the endocytosed DiI-OxLDL and the DAF had a large degree of overlap on intracellular vesicles (Fig. 7).

The failure of OxLDL to colocalize with caveolin-1 during endocytosis suggests that caveolae are not involved in OxLDL uptake. To directly address the requirement for caveolin-1/caveolae in the endocytosis of OxLDL through CD36, we studied the process in cell lines that lack caveolin-1. The mouse macrophage cell line J774 lacks caveolin-1 as assessed by Western blot (36, data not shown), and it was already shown that these cells can internalize OxLDL (Fig. 6*A*). However, because macrophages possess both the class B scavenger receptor CD36 and scavenger receptor class A (SR-A), another OxLDL receptor, it cannot be concluded from these data that OxLDL is internalized into J774 through CD36. SR-A and CD36 are the

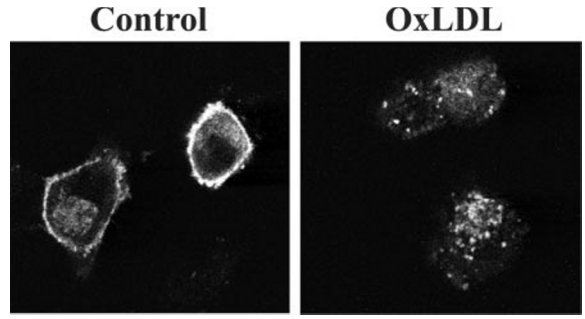

FIG. 8. **KB cells lacking caveolin-1 can internalize OxLDL through CD36.** KB cells, which lack caveolin-1, were transiently transfected with CD36-GFP. After 48 h, the cells were treated with OxLDL at 20 μg/ml or with buffer alone (control) for 1 h at 37 °C, then rinsed, fixed, and viewed by confocal fluorescence microscopy. CD36 has a plasma membrane distribution in the control cells but internalizes after treatment with OxLDL.

principal receptors responsible for the uptake of OxLDL in macrophages (37). To isolate the effect of CD36, the binding of OxLDL to J774 cells was done in the presence of the polyanions fucoidan or polyinosinic acid, which are inhibitors of SR-A but not CD36; the same pattern of uptake of OxLDL, albeit with reduced intensity, was seen (data not shown), suggesting that OxLDL uptake through CD36 can take place in cells lacking caveolin-1.

Next, endocytosis of OxLDL was studied in the KB cell line; these cells do not possess caveolin-1 or caveolae (data not shown). The KB cells were transiently transfected with CD36-GFP; 48 h later the cells were treated with OxLDL at 20 μg/ml for 1 h at 37 °C or with medium alone as a negative control. As viewed by confocal fluorescence microscopy, in the absence of OxLDL, the CD36-GFP was mainly localized on the plasma membrane, but following OxLDL exposure, the CD36-GFP was internalized into vesicles (Fig. 8).

DISCUSSION

The classic model of receptor-mediated endocytosis of macromolecules involves uptake through clathrin-coated pits, as exemplified by endocytosis via the LDL receptor or the transferrin receptor. More recent work has shown that this is just one of several pathways for endocytosis (35). Caveolae, another type of invagination or pit in the plasma membrane, had been implicated as a route for endocytosis (38). More recent studies of the endocytosis of albumin through gp60 (39, 40) and uptake of SV40 virus through caveolae (41) have shown that caveolae-mediated endocytosis is an alternate endocytic route that can lead to the pinching off of caveolae and their fusion with large intracellular vesicles termed caveosomes (41). The internalization of caveolae requires dynamin (42, 43), which is also required for clathrin-mediated endocytosis. Additional non-clathrin pathways have been described for the endocytosis of GPI-anchored proteins (44–46) and interleukin 2 (IL-2) (47). Both GPI-anchored proteins and the IL-2 receptor reside in lipid rafts, but the pathways for endocytosis of these two molecules do not appear to be identical, because GPI-anchored uptake is regulated by the Rho family GTPase cdc42 (46), whereas IL-2 endocytosis is regulated by the Rho family GTPase RhoA (47). It is not yet clear how many different types of endocytic vesicles exist in these non-clathrin pathways. For some of the ligands, such as SV40 virus, caveolin-1 is required (41), whereas for others, such as GPI-anchored proteins, caveolin-1 is not necessary for endocytosis (45). The non-clathrin, non-caveolar endocytosis is dependent on cholesterol and dynamin, but further details remain to be worked out on the molecular steps and the proteins required for this endocytic pathway (35, 48, 49).

Our studies were aimed at elucidating the endocytic process

responsible for the uptake of OxLDL through CD36. Initially, we utilized a combination of light and electron microscopy and biochemical analysis to confirm that CD36 was in rafts but that it was not in caveolae in the cells that we studied. This was established by the distinct patterns of expression of CD36 (homogeneous) *versus* caveolin-1 (punctate) on the plasma membrane, by the lack of colocalization of these two proteins by both fluorescence and electron microscopy, and by the lack of coimmunoprecipitation of CD36 and caveolin-1.

Our next studies looked at the endocytosis of OxLDL through CD36, and we established that OxLDL and CD36 are taken up into endocytic vesicles together and that the uptake process takes place in a similar manner in the heterologous system of human CD36 expressed in CHO cells as it does for CD36 endogenously expressed in the C32 human melanoma cell line and in the J774 mouse macrophage cell line. This latter cell line is relevant because of the role of macrophages in the uptake of OxLDL in a process that produces lipid-laden foam cells (50). To determine the specific pathway of endocytosis, we utilized dual fluorescence markers to simultaneously study the internalization of OxLDL (DiI-labeled) with either caveolin-1, transferrin, or the GPI-anchored protein DAF, which serve as markers of caveolar-mediated, clathrin-mediated, or raft-mediated endocytic pathways, respectively. OxLDL was clearly endocytosed through a non-clathrin, non-caveolar, raft-mediated pathway, showing extensive endocytosis into the same vesicles as DAF.

We found no evidence for a required role for caveolin-1 and caveolae in the endocytosis of OxLDL through CD36. First, as discussed above, there was no colocalization of OxLDL and caveolin-1 during endocytosis. Second, the uptake of OxLDL occurred in the caveolin-1-negative J774 cell line, even when uptake through SR-A was blocked. Third, there was endocytosis of OxLDL in the KB cell line transfected with CD36, although KB cells do not express caveolin-1 or caveolae. Thus, it is clear that caveolin-1 is not required for endocytosis of OxLDL through CD36. In a recent report, caveolin-1 was immunopurified from adipocytes, and CD36 was one of the proteins that copurified with caveolin-1 (51). It is notable that adipocytes are the tissue with the highest level of caveolin-1 expression (52). The partitioning of plasma membrane proteins between the non-raft domain, rafts (excluding caveolae), and caveolae is a dynamic process; the distribution of CD36 could vary depending on the levels of caveolae in different cells. Nonetheless, our results demonstrate that the endocytosis of OxLDL through CD36 occurs via a raft-mediated pathway and that caveolae are not necessary for the process. Whether caveolin-1 could modulate the endocytosis of OxLDL under some circumstances remains to be determined.

The delineation of this raft pathway for endocytosis of OxLDL through CD36 will provide the basis for future studies of the detailed molecular mechanisms and regulatory molecules that control this process. Given the key role of OxLDL endocytosis in macrophages as an early step in atherosclerosis, this endocytic pathway will be an important target of future investigations.

Acknowledgment—We thank Marilyn Levy for expert assistance with electron microscopy.

REFERENCES

1. Tandon, N. N., Lipsky, R. H., Burgess, W. H., and Jamieson, G. A. (1989) *J. Biol. Chem.* **264,** 7570–7575
2. Silverstein, R. L., Asch, A. S., and Nachman, R. L. (1989) *J. Clin. Invest.* **84,** 546–552
3. Greenwalt, D. E., Watt, K. W., So, O. Y., and Jiwani, N. (1990) *Biochemistry* **29,** 7054–7059
4. Knowles, D. M., 2nd, Tolidjian, B., Marboe, C., D'Agati, V., Grimes, M., and Chess, L. (1984) *J. Immunol.* **132,** 2170–2173
5. Abumrad, N. A., el-Maghrabi, M. R., Amri, E. Z., Lopez, E., and Grimaldi, P. A. (1993) *J. Biol. Chem.* **268,** 17665–17668
6. Asch, A. S., Barnwell, J., Silverstein, R. L., and Nachman, R. L. (1987) *J. Clin. Invest.* **79,** 1054–1061
7. Endemann, G., Stanton, L. W., Madden, K. S., Bryant, C. M., White, R. T., and Protter, A. A. (1993) *J. Biol. Chem.* **268,** 11811–11816
8. Nicholson, A. C., Frieda, S., Pearce, A., and Silverstein, R. L. (1995) *Arterioscler. Thromb. Vasc. Biol.* **15,** 269–275
9. Rigotti, A., Acton, S. L., and Krieger, M. (1995) *J. Biol. Chem.* **270,** 16221–16224
10. Savill, J., Hogg, N., Ren, Y., and Haslett, C. (1992) *J. Clin. Invest.* **90,** 1513–1522
11. Ren, Y., Silverstein, R. L., Allen, J., and Savill, J. (1995) *J. Exp. Med.* **181,** 1857–1862
12. Oquendo, P., Hundt, E., Lawler, J., and Seed, B. (1989) *Cell* **58,** 95–101
13. Febbraio, M., Hajjar, D. P., and Silverstein, R. L. (2001) *J. Clin. Invest.* **108,** 785–791
14. Glass, C. K., and Witztum, J. L. (2001) *Cell* **104,** 503–516
15. Nozaki, S., Kashiwagi, H., Yamashita, S., Nakagawa, T., Kostner, B., Tomiyama, Y., Nakata, A., Ishigami, M., Miyagawa, J., and Kameda-Takemura, K., Kurata, Y., and Matsuzawa, Y. (1995) *J. Clin. Invest.* **96,** 1859–1865
16. Febbraio, M., Podrez, E. A., Smith, J. D., Hajjar, D. P., Hazen, S. L., Hoff, H. F., Sharma, K., and Silverstein, R. L. (2000) *J. Clin. Invest.* **105,** 1049–1056
17. Lisanti, M. P., Scherer, P. E., Vidugiriene, J., Tang, Z., Hermanowski-Vosatka, A., Tu, Y. H., Cook, R. F., and Sargiacomo, M. (1994) *J. Cell Biol.* **126,** 111–126
18. Brown, D. A., and London, E. (2000) *J. Biol. Chem.* **275,** 17221–17224
19. Simons, K., and Toomre, D. (2000) *Nat. Rev. Mol. Cell Biol.* **1,** 31–39
20. Razani, B., Woodman, S. E., and Lisanti, M. P. (2002) *Pharmacol. Rev.* **54,** 431–467
21. Rothberg, K. G., Heuser, J. E., Donzell, W. C., Ying, Y. S., Glenney, J. R., and Anderson, R. G. (1992) *Cell* **68,** 673–682
22. Fra, A. M., Williamson, E., Simons, K., and Parton, R. G. (1995) *Proc. Natl. Acad. Sci. U. S. A.* **92,** 8655–8659
23. Drab, M., Verkade, P., Elger, M., Kasper, M., Lohn, M., Lauterbach, B., Menne, J., Lindschau, C., Mende, F., Luft, F. C., Schedl, A., Haller, H., and Kurzchalia, T. V. (2001) *Science* **293,** 2449–2452
24. Razani, B., Engelman, J. A., Wang, X. B., Schubert, W., Zhang, X. L., Marks, C. B., Macaluso, F., Russell, R. G., Li, M., Pestell, R. G., Di Vizio, D., Hou, H., Jr., Kneitz, B., Lagaud, G., Christ, G. J., Edelmann, W., and Lisanti, M. P. (2001) *J. Biol. Chem.* **276,** 38121–38138
25. Brown, D. A., and Rose, J. K. (1992) *Cell* **68,** 533–544
26. Sargiacomo, M., Sudol, M., Tang, Z., and Lisanti, M. P. (1993) *J. Cell Biol.* **122,** 789–807
27. Lublin, D. M., and Coyne, K. E. (1991) *J. Exp. Med.* **174,** 35–44
28. Coyne, K. E., Hall, S. E., Thompson, S., Arce, M. A., Kinoshita, T., Fujita, T., Anstee, D. J., Rosse, W., and Lublin, D. M. (1992) *J. Immunol.* **149,** 2906–2913
29. Tao, N., Wagner, S. J., and Lublin, D. M. (1996) *J. Biol. Chem.* **271,** 22315–22320
30. Dietzen, D. J., Hastings, W. R., and Lublin, D. M. (1995) *J. Biol. Chem.* **270,** 6838–6842
31. Griffiths, G., McDowall, A., Back, R., and Dubochet, J. (1984) *J. Ultrastruct. Res.* **89,** 65–78
32. Thorne, R. F., Marshall, J. F., Shafren, D. R., Gibson, P. G., Hart, I. R., and Burns, G. F. (2000) *J. Biol. Chem.* **275,** 35264–35275
33. London, E., and Brown, D. A. (2000) *Biochim. Biophys. Acta* **1508,** 182–195
34. Scherer, P. E., Lewis, R. Y., Volonte, D., Engelman, J. A., Galbiati, F., Couet, J., Kohtz, D. S., van Donselaar, E., Peters, P., and Lisanti, M. P. (1997) *J. Biol. Chem.* **272,** 29337–29346
35. Conner, S. D., and Schmid, S. L. (2003) *Nature* **422,** 37–44
36. Gargalovic, P., and Dory, L. (2001) *J. Biol. Chem.* **276,** 26164–26170
37. Kunjathoor, V. V., Febbraio, M., Podrez, E. A., Moore, K. J., Andersson, L., Koehn, S., Rhee, J. S., Silverstein, R., Hoff, H. F., and Freeman, M. W. (2002) *J. Biol. Chem.* **277,** 49982–49988
38. Montesano, R., Roth, J., Robert, A., and Orci, L. (1982) *Nature* **296,** 651–653
39. Schnitzer, J. E., Oh, P., Pinney, E., and Allard, J. (1994) *J. Cell Biol.* **127,** 1217–1232
40. Schubert, W., Frank, P. G., Razani, B., Park, D. S., Chow, C. W., and Lisanti, M. P. (2001) *J. Biol. Chem.* **276,** 48619–48622
41. Pelkmans, L., Kartenbeck, J., and Helenius, A. (2001) *Nat. Cell Biol.* **3,** 473–483
42. Oh, P., McIntosh, D. P., and Schnitzer, J. E. (1998) *J. Cell Biol.* **141,** 101–114
43. Pelkmans, L., Puntener, D., and Helenius, A. (2002) *Science* **296,** 535–539
44. Nichols, B. J., Kenworthy, A. K., Polishchuk, R. S., Lodge, R., Roberts, T. H., Hirschberg, K., Phair, R. D., and Lippincott-Schwartz, J. (2001) *J. Cell Biol.* **153,** 529–541
45. Nichols, B. J. (2002) *Nat. Cell Biol.* **4,** 374–378
46. Sabharanjak, S., Sharma, P., Parton, R. G., and Mayor, S. (2002) *Dev. Cell* **2,** 411–423
47. Lamaze, C., Dujeancourt, A., Baba, T., Lo, C. G., Benmerah, A., and Dautry-Varsat, A. (2001) *Mol. Cell* **7,** 661–671
48. Nichols, B. J., and Lippincott-Schwartz, J. (2001) *Trends Cell Biol.* **11,** 406–412
49. Nabi, I. R., and Le, P. U. (2003) *J. Cell Biol.* **161,** 673–677
50. Goldstein, J. L., Ho, Y. K., Basu, S. K., and Brown, M. S. (1979) *Proc. Natl. Acad. Sci. U. S. A.* **76,** 333–337
51. Souto, R. P., Vallega, G., Wharton, J., Vinten, J., Tranum-Jensen, J., and Pilch, P. F. (2003) *J. Biol. Chem.* **278,** 18321–18329
52. Scherer, P. E., Lisanti, M. P., Baldini, G., Sargiacomo, M., Mastick, C. C., and Lodish, H. F. (1994) *J. Cell Biol.* **127,** 1233–1243